SIAM J. SCI. COMPUT.
Vol. 25, No. 6, pp. 2050–2065

A FAST AND STABLE WELL-BALANCED SCHEME WITH HYDROSTATIC RECONSTRUCTION FOR SHALLOW WATER FLOWS*

EMMANUEL AUDUSSE†, FRANÇOIS BOUCHUT‡, MARIE-ODILE BRISTEAU†, RUPERT KLEIN§, AND BENOÎT PERTHAME†‡

Abstract. We consider the Saint-Venant system for shallow water flows, with nonflat bottom. It is a hyperbolic system of conservation laws that approximately describes various geophysical flows, such as rivers, coastal areas, and oceans when completed with a Coriolis term, or granular flows when completed with friction. Numerical approximate solutions to this system may be generated using conservative finite volume methods, which are known to properly handle shocks and contact discontinuities. However, in general these schemes are known to be quite inaccurate for near steady states, as the structure of their numerical truncation errors is generally not compatible with exact physical steady state conditions. This difficulty can be overcome by using the so-called well-balanced schemes. We describe a general strategy, based on a local hydrostatic reconstruction, that allows us to derive a well-balanced scheme from any given numerical flux for the homogeneous problem. Whenever the initial solver satisfies some classical stability properties, it yields a simple and fast well-balanced scheme that preserves the nonnegativity of the water height and satisfies a semidiscrete entropy inequality.

Key words. shallow water equations, finite volume schemes, well-balanced schemes

AMS subject classifications. 65M12, 76M12, 35L65

DOI. 10.1137/S1064827503431090

1. Introduction.

The classical Saint-Venant system for shallow water has been widely validated. It assumes a slowly varying topography $z(x)$ (x denotes a coordinate in the horizontal direction) and describes the height of water $h(t,x)$ and the water velocity $u(t,x)$ in the direction parallel to the bottom. It uses the following equations in one space dimension:

$$\begin{cases} \partial_t h + \partial_x(hu) = 0, \\ \partial_t(hu) + \partial_x(hu^2 + gh^2/2) = -hgz_x, \end{cases} \tag{1.1}$$

where $g > 0$ denotes the gravity constant. For future reference we denote the flux by $F(U) = (hu, hu^2 + gh^2/2)$, with $U = (h, hu)$. This model is very robust, being hyperbolic and admitting an entropy inequality (related to the physical energy)

$$\partial_t \widetilde{\eta}(U,z) + \partial_x \widetilde{G}(U,z) \le 0, \tag{1.2}$$

*Received by the editors July 4, 2003; accepted for publication (in revised form) October 30, 2003; published electronically June 25, 2004. This work was partially supported by the ACI Modélisation de processus hydrauliques à surface libre en présence de singularités (http://www-rocq.inria.fr/m3n/CatNat/), by HYKE European programme HPRN-CT-2002-00282 (http://www.hyke.org), by EDF/LNHE (E.A., F.B., M.-O.B., B.P.), and by grant KL 611/6 of the Deutsche Forschungsgemeinschaft (R.K.).

http://www.siam.org/journals/sisc/25-6/43109.html

†INRIA Rocquencourt, projet BANG, Domaine de Voluceau, BP 105, 78153 Le Chesnay cedex, France (emmanuel.audusse@inria.fr, marie-odile.bristeau@inria.fr).

‡Département de Mathématiques et Applications, CNRS & École Normale Supérieure, 45 rue d'Ulm, F 75230 Paris cedex 05, France (fbouchut@dma.ens.fr, perthame@dma.ens.fr).

§Department of Mathematics and Computer Science, Freie Universität Berlin, D-14195 Berlin, Germany (rupert.klein@zib.de).

where

$$\eta(U) = hu^2/2 + \frac{g}{2}h^2, \qquad G(U) = \left(hu^2/2 + gh^2\right)u, \tag{1.3}$$
$$\widetilde{\eta}(U,z) = \eta(U) + hgz, \qquad \widetilde{G}(U,z) = G(U) + hgzu.$$

Another nice property is that it preserves the steady state of a lake at rest:

$$h + z = Cst, \qquad u = 0. \tag{1.4}$$

When solving (1.1) numerically, it is very important to be able to preserve these steady states at the discrete level and to accurately compute the evolution of small deviations from them, because the majority of real-life applications resides in this flow regime. Other steady states with nonvanishing velocity can also be considered, but we shall not do so in the present work.

Since the early works of LeRoux and coauthors [14], [16], schemes satisfying such a property have been called well-balanced. Several schemes have been proposed that satisfy this property (exactly or at least at second-order) [24], [18], [13], [11], [32], [31], [3]. But the difficulty is then to get schemes that also satisfy very natural properties, such as conservativity of the water height h, nonnegativity of h, to compute dry states $h = 0$ and transcritical flows when the Jacobian matrix F' of the flux function becomes singular (this difficulty is related to resonance, and theoretical studies can be found, for instance, in [25], [17]), and eventually to satisfy a discrete entropy inequality. This last property ensures the admissibility of shocks and gives overall the nonlinear stability of the scheme. Theoretically, the exact Godunov scheme satisfies these requirements [21], but it is in practice computationally too expensive, and not easily adaptable to more complex systems, such as, for example, the models proposed in [9]. The first attempt to derive an approximate solver satisfying all the requirements was performed in [4] for a scalar equation (in this case, only the ability to treat transcritical flows with an entropy inequality is meaningful, together with the well-balanced property). A generalization to the case of the Saint-Venant system was obtained in [28], and another method by relaxation is also proposed in [7]. However, these approximate solver methods are still quite heavy in practice. The aim of this paper is to explain how it is possible, by a very flexible approach involving a hydrostatic reconstruction, to obtain a well-balanced scheme satisfying all the above requirements, and which is computationally inexpensive. The present approach unifies and generalizes ideas developed independently in [5], [6] for nearly hydrostatic, multidimensional compressible flow, and in [1] for the Saint-Venant shallow water model. In contrast with the above-mentioned methods [28], [7], it is generic in the sense that it can be used in conjunction with any given numerical flux for the homogeneous (i.e., with constant topography) Saint-Venant problem.

2. Well-balanced scheme with hydrostatic reconstruction.

2.1. Semidiscrete scheme. Finite volume schemes for hyperbolic systems consist in using an upwinding of the fluxes. In the semidiscrete case they provide a discrete version of (1.1) under the form

$$\Delta x_i \frac{d}{dt} U_i(t) + F_{i+1/2} - F_{i-1/2} = S_i, \tag{2.1}$$

where Δx_i denotes a possibly variable mesh size $\Delta x_i = x_{i+1/2} - x_{i-1/2}$, and the cell-centered vector of discrete unknowns is

$$U_i(t) = \begin{pmatrix} h_i(t) \\ h_i(t)u_i(t) \end{pmatrix}. \tag{2.2}$$

In a basic first-order accurate scheme, the fluxes are classically computed as $F_{i+1/2} = \mathcal{F}(U_i(t), U_{i+1}(t))$ with a numerical flux $\mathcal{F}$ that is computed via an approximate resolution of the Riemann problem (a so-called *solver*), which provides stability of the method. We refer to [12] for descriptions of the most well-known solvers: Godunov, Roe, Kinetic, etc. It is known since [14], [16] that cell-centered evaluations of the source term in (2.1) will generally not be able to maintain in time steady states of a lake at rest, which are characterized by

$$h_i + z_i = Cst, \qquad u_i = 0. \tag{2.3}$$

Following [1], [5], [6], we propose and analyze finite volume schemes according to (2.1) with flux functions

$$F_{i+1/2} = \mathcal{F}(U_{i+1/2-}, U_{i+1/2+}), \tag{2.4}$$

where the interface values $U_{i+1/2-}, U_{i+1/2+}$ are derived from a local hydrostatic reconstruction to be described shortly, which is similar to second-order reconstructions in higher-order methods. The source term is discretized as

$$S_i = \begin{pmatrix} 0 \\ \frac{g}{2} h_{i+1/2-}^2 - \frac{g}{2} h_{i-1/2+}^2 \end{pmatrix}. \tag{2.5}$$

This ansatz is motivated by a balancing requirement, as follows. For nearly hydrostatic flows one has $u \ll \sqrt{gh}$. In the associated asymptotic limit the leading order water height $\underline{h}$ adjusts so as to satisfy the balance of momentum flux and momentum source terms, i.e.,

$$\partial_x \left(\frac{g\underline{h}^2}{2} \right) = -\underline{h}\, g z_x \,. \tag{2.6}$$

Integrating over, say, the ith grid cell we obtain an approximation to the net source term as

$$-\int_{x_{i-1/2}}^{x_{i+1/2}} \underline{h}\, g z_x \, dx = \frac{g}{2} \underline{h}_{i+1/2-}^2 - \frac{g}{2} \underline{h}_{i-1/2+}^2 \,. \tag{2.7}$$

Thus we are able to locally represent the cell-averaged source term as the discrete gradient of the hydrostatic momentum flux, and this motivates the source term discretization in (2.5).

It is obvious now that any hydrostatic state is maintained exactly if, for such a state, the momentum fluxes in (2.1) and the locally reconstructed heights satisfy $F_{i+1/2}^{hu} = \frac{1}{2} g h_{i+1/2-}^2 = \frac{1}{2} g h_{i+1/2+}^2$. This is the motivation for (2.4), which gives this property if, for hydrostatic states, we have $U_{i+1/2-} = U_{i+1/2+} = (h_{i+1/2-}, 0) = (h_{i+1/2+}, 0)$.

The hydrostatic balance in (2.6) is equivalent to the "lake at rest" equation (1.4), so that the reconstruction of the leading order heights is straightforward:

$$\underline{h}_{i+1/2-} = h_i + z_i - z_{i+1/2}, \qquad \underline{h}_{i+1/2+} = h_{i+1} + z_{i+1} - z_{i+1/2}. \tag{2.8}$$

An important challenge is to design a scheme that robustly captures dry regions where $h \equiv 0$. In order to ensure nonnegativity of the water height even when cells begin to

"dry out," we need first to perform a truncation of the leading order heights in (2.8), $h_{i+1/2\pm} = \max(0, \underline{h}_{i+1/2\pm})$. Next, the evaluation of the cell interface height $z_{i+1/2}$ has to be done in a quite subtle way. Our construction, combined with a centered value of $z_{i+1/2}$, is not stable. We rather take an *upwind* evaluation of the form

$$z_{i+1/2} = \max(z_i, z_{i+1}). \tag{2.9}$$

With these choices, we ensure that $0 \le h_{i+1/2-} \le h_i$ and $0 \le h_{i+1/2+} \le h_{i+1}$, and we prove below that this property ensures the nonnegativity requirement.

With these rules in place we can now summarize our first-order well-balanced finite volume scheme by

$$\Delta x_i \frac{d}{dt} U_i(t) + F_{i+1/2} - F_{i-1/2} = S_i, \tag{2.10}$$

where

$$F_{i+1/2} = \mathcal{F}(U_{i+1/2-}, U_{i+1/2+}), \tag{2.11}$$

$$U_{i+1/2-} = \begin{pmatrix} h_{i+1/2-} \\ h_{i+1/2-}\, u_i \end{pmatrix}, \qquad U_{i+1/2+} = \begin{pmatrix} h_{i+1/2+} \\ h_{i+1/2+}\, u_{i+1} \end{pmatrix}, \tag{2.12}$$

$$h_{i+1/2-} = \max(0, h_i + z_i - z_{i+1/2}), \qquad h_{i+1/2+} = \max(0, h_{i+1} + z_{i+1} - z_{i+1/2}), \tag{2.13}$$

and

$$S_i = S_{i+1/2-} + S_{i-1/2+} \equiv \begin{pmatrix} 0 \\ \frac{g}{2} h_{i+1/2-}^2 - \frac{g}{2} h_i^2 \end{pmatrix} + \begin{pmatrix} 0 \\ \frac{g}{2} h_i^2 - \frac{g}{2} h_{i-1/2+}^2 \end{pmatrix}. \tag{2.14}$$

The latter expression for the source is equivalent to the earlier (2.5); it shows that the source may be considered as being distributed to the cell interfaces. With this reinterpretation in mind, we may also rewrite the scheme as

$$\Delta x_i \frac{d}{dt} U_i(t) + \mathcal{F}_l(U_i, U_{i+1}, z_i, z_{i+1}) - \mathcal{F}_r(U_{i-1}, U_i, z_{i-1}, z_i) = 0, \tag{2.15}$$

with left and right numerical fluxes,

$$\begin{aligned} \mathcal{F}_l(U_i, U_{i+1}, z_i, z_{i+1}) &= F_{i+1/2} - S_{i+1/2-} \\ &= \mathcal{F}(U_{i+1/2-}, U_{i+1/2+}) + \begin{pmatrix} 0 \\ \frac{g}{2} h_i^2 - \frac{g}{2} h_{i+1/2-}^2 \end{pmatrix}, \\ \mathcal{F}_r(U_i, U_{i+1}, z_i, z_{i+1}) &= F_{i+1/2} + S_{i+1/2+} \\ &= \mathcal{F}(U_{i+1/2-}, U_{i+1/2+}) + \begin{pmatrix} 0 \\ \frac{g}{2} h_{i+1}^2 - \frac{g}{2} h_{i+1/2+}^2 \end{pmatrix}. \end{aligned} \tag{2.16}$$

Our construction is reminiscent of the formulas proposed in [16], [14], [13] using the full steady state equations to compute intermediate states at which the numerical flux is evaluated. The difference is that here, (2.12), (2.13) mean that we try to impose interface values satisfying some modified steady equations $h_{i+1/2-} + z_{i+1/2} = h_i + z_i$, $u_{i+1/2-} = u_i$, $h_{i+1/2+} + z_{i+1/2} = h_{i+1} + z_{i+1}$, $u_{i+1/2+} = u_{i+1}$, i.e., $h + z = cst$, $u = cst$ instead of Bernoulli's law $u^2/2 + g(h + z) = cst$, $hu = cst$. The advantage of

these new relations is that now we have no singularity at critical points (observe that the numerical fluxes $\mathcal{F}_l$, $\mathcal{F}_r$ depend continuously on the data), while these relations coincide with the exact ones in the case of interest: $u = 0$ corresponding to (2.3). Strikingly, this modification does not affect the consistency of the scheme, even in far from steady situations.

THEOREM 2.1. *Consider a consistent numerical flux $\mathcal{F}$ for the homogeneous problem that preserves nonnegativity of $h_i(t)$ and satisfies an in-cell entropy inequality corresponding to the entropy η in* (1.3)*. Then the finite volume scheme* (2.9)–(2.14)

(i) *preserves the nonnegativity of $h_i(t)$;*
(ii) *is well-balanced, i.e., preserves the steady state of a lake at rest* (2.3)*;*
(iii) *is consistent with the Saint-Venant system* (1.1)*;*
(iv) *satisfies an in-cell entropy inequality associated to the entropy $\widetilde{\eta}$ in* (1.3)*,*

$$\Delta x_i \frac{d}{dt}\widetilde{\eta}(U_i(t), z_i) + \widetilde{G}_{i+1/2} - \widetilde{G}_{i-1/2} \leq 0. \tag{2.17}$$

Proof. (i) The statement that $\mathcal{F}$ preserves the nonnegativity of $h_i(t)$ means exactly that $\mathcal{F}^h(h_i = 0, u_i, h_{i+1}, u_{i+1}) - \mathcal{F}^h(h_{i-1}, u_{i-1}, h_i = 0, u_i) \leq 0$ for all choices of the other arguments. Since the sources in (2.14) have no contribution to the first component, $h_i(t)$ in our scheme satisfies a conservative equation with flux $\mathcal{F}^h(U_{i+1/2-}, U_{i+1/2+})$. Therefore we need to check that $\mathcal{F}^h(U_{i+1/2-}, U_{i+1/2+}) - \mathcal{F}^h(U_{i-1/2-}, U_{i-1/2+}) \leq 0$ whenever $h_i = 0$. As mentioned above, our construction (2.9), (2.13) ensures that $h_{i+1/2-} \leq h_i$ and $h_{i+1/2+} \leq h_{i+1}$, and thus $h_{i+1/2-} = h_{i-1/2+} = 0$ when $h_i = 0$, and this gives (i).

(ii) On a steady state of a lake at rest, we have $h_{i+1/2-} = h_{i+1/2+}$, $u_{i+1} = u_i = 0$, and thus $U_{i+1/2-} = U_{i+1/2+}$ and by consistency of $\mathcal{F}$

$$F_{i+1/2} = F(U_{i+1/2-}) = F(U_{i+1/2+}) = \begin{pmatrix} 0 \\ \frac{g}{2}h_{i+1/2-}^2 \end{pmatrix} = \begin{pmatrix} 0 \\ \frac{g}{2}h_{i+1/2+}^2 \end{pmatrix}. \tag{2.18}$$

Together with the expression of the source terms in (2.14), we get $\mathcal{F}_l = F_{i+1/2} - S_{i+1/2-} = F(U_i)$, $\mathcal{F}_r = F_{i+1/2} + S_{i+1/2+} = F(U_{i+1})$, and this proves (ii).

(iii) To prove (iii), we apply the criterion in [29], [7], and we need to check two properties related to the consistency with the exact flux F and the consistency with the source. The consistency with the exact flux $\mathcal{F}_l(U, U, z, z) = \mathcal{F}_r(U, U, z, z) = F(U)$ is obvious since $U_{i+1/2-} = U_i$ and $U_{i+1/2+} = U_{i+1}$ whenever $z_{i+1} = z_i$. For consistency with the source, the criterion becomes for the Saint-Venant system

$$\mathcal{F}_r^{hu}(U_i, U_{i+1}, z_i, z_{i+1}) - \mathcal{F}_l^{hu}(U_i, U_{i+1}, z_i, z_{i+1}) = -hg\Delta z_{i+1/2} + o(\Delta z_{i+1/2}), \tag{2.19}$$

as $U_i, U_{i+1} \to U$ and $\Delta z_{i+1/2} \to 0$, where $\Delta z_{i+1/2} = z_{i+1} - z_i$. In our case,

$$\mathcal{F}_r - \mathcal{F}_l = S_{i+1/2-} + S_{i+1/2+} = \begin{pmatrix} 0 \\ \frac{g}{2}h_{i+1/2-}^2 - \frac{g}{2}h_i^2 + \frac{g}{2}h_{i+1}^2 - \frac{g}{2}h_{i+1/2+}^2 \end{pmatrix}. \tag{2.20}$$

Now, assuming $h > 0$, the maxima in (2.13) play no role if $h_i - h$, $h_{i+1} - h$, and $\Delta z_{i+1/2}$ are small enough. Thus we have $h_{i+1/2-}^2/2 - h_i^2/2 = h(z_i - z_{i+1/2}) + o(\Delta z_{i+1/2})$, $h_{i+1/2+}^2/2 - h_{i+1}^2/2 = h(z_{i+1} - z_{i+1/2}) + o(\Delta z_{i+1/2})$, which gives (2.19). In the special case $h = 0$, the maxima in (2.13) can play a role only when $h_i = O(\Delta z_{i+1/2})$, and we conclude that (2.19) always holds, proving (iii).

(iv) In order to prove (iv), we first write that the original numerical flux $\mathcal{F}$ satisfies a semidiscrete entropy inequality. According to [7], this means that we can find a numerical entropy flux $\mathcal{G}$ such that

$$\begin{aligned} &G(U_{i+1}) + \eta'(U_{i+1})(\mathcal{F}(U_i, U_{i+1}) - F(U_{i+1})) \\ &\le \mathcal{G}(U_i, U_{i+1}) \le G(U_i) + \eta'(U_i)(\mathcal{F}(U_i, U_{i+1}) - F(U_i)), \end{aligned} \tag{2.21}$$

where η' is the derivative of η with respect to $U = (h, hu)$, $\eta'(U) = (gh - u^2/2, u)$. Similarly, having an entropy inequality (2.17) for (1.1) with $\widetilde{G}_{i+1/2} = \widetilde{\mathcal{G}}(U_i, U_{i+1}, z_i, z_{i+1})$ is equivalent to finding some numerical entropy flux $\widetilde{\mathcal{G}}$ such that

$$\begin{aligned} &\widetilde{G}(U_{i+1}, z_{i+1}) + \widetilde{\eta}'(U_{i+1}, z_{i+1})(\mathcal{F}_r(U_i, U_{i+1}, z_i, z_{i+1}) - F(U_{i+1})) \\ &\le \widetilde{\mathcal{G}}(U_i, U_{i+1}, z_i, z_{i+1}) \le \widetilde{G}(U_i, z_i) + \widetilde{\eta}'(U_i, z_i)(\mathcal{F}_l(U_i, U_{i+1}, z_i, z_{i+1}) - F(U_i)). \end{aligned} \tag{2.22}$$

Let us prove that (2.22) holds with

$$\widetilde{\mathcal{G}}(U_i, U_{i+1}, z_i, z_{i+1}) = \mathcal{G}(U_{i+1/2-}, U_{i+1/2+}) + \mathcal{F}^h(U_{i+1/2-}, U_{i+1/2+}) g z_{i+1/2}. \tag{2.23}$$

Since both inequalities are obtained by the same type of estimates, let us prove only the upper inequality involving $\mathcal{F}_l$ in (2.22). By comparison to (2.21), it is enough to prove that

$$\begin{aligned} &G(U_{i+1/2-}) + \eta'(U_{i+1/2-})\big(\mathcal{F}(U_{i+1/2-}, U_{i+1/2+}) - F(U_{i+1/2-})\big) \\ &\quad + \mathcal{F}^h(U_{i+1/2-}, U_{i+1/2+}) g z_{i+1/2} \\ &\le G(U_i) + \eta'(U_i)(\mathcal{F}_l - F(U_i)) + \mathcal{F}^h(U_{i+1/2-}, U_{i+1/2+}) g z_i. \end{aligned} \tag{2.24}$$

This inequality can be written, by denoting $\mathcal{F} = (\mathcal{F}^h, \mathcal{F}^{hu}) = \mathcal{F}(U_{i+1/2-}, U_{i+1/2+})$, as

$$\begin{aligned} &(u_i^2/2 + g h_{i+1/2-}) h_{i+1/2-} u_i + (g h_{i+1/2-} - u_i^2/2)(\mathcal{F}^h - h_{i+1/2-} u_i) \\ &\quad + u_i(\mathcal{F}^{hu} - h_{i+1/2-} u_i^2 - g h_{i+1/2-}^2/2) + \mathcal{F}^h g(z_{i+1/2} - z_i) \\ &\le (u_i^2/2 + g h_i) h_i u_i + (g h_i - u_i^2/2)(\mathcal{F}^h - h_i u_i) + u_i(\mathcal{F}_l^{hu} - h_i u_i^2 - g h_i^2/2), \end{aligned} \tag{2.25}$$

or, after simplification,

$$u_i(\mathcal{F}^{hu} - g h_{i+1/2-}^2/2) + \mathcal{F}^h g(h_{i+1/2-} - h_i + z_{i+1/2} - z_i) \le u_i(\mathcal{F}_l^{hu} - g h_i^2/2). \tag{2.26}$$

Since $\mathcal{F}_l^{hu} - g h_i^2/2 = \mathcal{F}^{hu} - g h_{i+1/2-}^2/2$ by definition of $\mathcal{F}_l$ in (2.16), our inequality finally reduces to

$$\mathcal{F}^h(U_{i+1/2-}, U_{i+1/2+})(h_{i+1/2-} - h_i + z_{i+1/2} - z_i) \le 0. \tag{2.27}$$

Now, according to (2.13), when this quantity is nonzero, we have $h_{i+1/2-} = 0$ and the expression between parentheses is nonnegative. But since $\mathcal{F}$ preserves nonnegativity, we have $\mathcal{F}^h(h_{i+1/2-} = 0, u_i, h_{i+1/2+}, u_{i+1}) \le 0$, and we conclude that (2.27) always holds. This completes the proof of (iv). ∎

2.2. Fully discrete scheme and CFL condition. When using the time-space fully discrete scheme

$$U_i^{n+1} - U_i^n + \frac{\Delta t}{\Delta x_i}\Big(\mathcal{F}_l(U_i, U_{i+1}, z_i, z_{i+1}) - \mathcal{F}_r(U_{i-1}, U_i, z_{i-1}, z_i)\Big) = 0, \tag{2.28}$$

the consistency and the well-balanced property are of course still valid. The question is then to obtain a CFL condition that guarantees stability.

One can prove that our hydrostatic reconstruction scheme does not satisfy a fully discrete entropy inequality. Indeed there exist some data with $h_i + z_i = cst$, $u_i = cst \neq 0$ such that for any $\Delta t > 0$, the fully discrete entropy inequality $\widetilde{\eta}(U_i^{n+1}, z_i) - \widetilde{\eta}(U_i^n, z_i) + \frac{\Delta t}{\Delta x_i}(\widetilde{G}_{i+1/2} - \widetilde{G}_{i-1/2}) \leq 0$ is violated. However, these data are not preserved by the scheme. The consequence is that in practice we do not observe instabilities as long as the water height h_i remains nonnegative.

In order to preserve the nonnegativity of h_i, the CFL condition that needs to be used is not more restrictive than that of the homogeneous solver.

PROPOSITION 2.2. *Assume that the homogeneous flux $\mathcal{F}$ preserves the nonnegativity of h* by interface *with a numerical speed $\sigma(U_i, U_{i+1}) \geq 0$, which means that whenever the CFL condition*

$$\sigma(U_i, U_{i+1})\Delta t \leq \min(\Delta x_i, \Delta x_{i+1}) \tag{2.29}$$

holds, we have

$$\begin{aligned} &h_i - \frac{\Delta t}{\Delta x_i}(\mathcal{F}^h(U_i, U_{i+1}) - h_i u_i) \geq 0, \\ &h_{i+1} - \frac{\Delta t}{\Delta x_{i+1}}(h_{i+1}u_{i+1} - \mathcal{F}^h(U_i, U_{i+1})) \geq 0. \end{aligned} \tag{2.30}$$

Then the fully discrete hydrostatic reconstruction scheme (2.28) *also preserves the nonnegativity of h* by interface*,*

$$\begin{aligned} &h_i - \frac{\Delta t}{\Delta x_i}(\mathcal{F}^h(U_{i+1/2-}, U_{i+1/2+}) - h_i u_i) \geq 0, \\ &h_{i+1} - \frac{\Delta t}{\Delta x_{i+1}}(h_{i+1}u_{i+1} - \mathcal{F}^h(U_{i+1/2-}, U_{i+1/2+})) \geq 0, \end{aligned} \tag{2.31}$$

under the CFL condition

$$\sigma(U_{i+1/2-}, U_{i+1/2+})\Delta t \leq \min(\Delta x_i, \Delta x_{i+1}). \tag{2.32}$$

Proof. Under the CFL condition (2.32), we have

$$\begin{aligned} &h_{i+1/2-} - \frac{\Delta t}{\Delta x_i}(\mathcal{F}^h(U_{i+1/2-}, U_{i+1/2+}) - h_{i+1/2-}u_{i+1/2-}) \geq 0, \\ &h_{i+1/2+} - \frac{\Delta t}{\Delta x_{i+1}}(h_{i+1/2+}u_{i+1/2+} - \mathcal{F}^h(U_{i+1/2-}, U_{i+1/2+})) \geq 0. \end{aligned} \tag{2.33}$$

As previously mentioned, with the choice (2.9), (2.13), we have $h_{i+1/2-} \leq h_i$ and $h_{i+1/2+} \leq h_{i+1}$. Thus we deduce that (2.31) holds as soon as $1 + u_i\Delta t/\Delta x_i \geq 0$ and $1 - u_{i+1}\Delta t/\Delta x_{i+1} \geq 0$, which is necessarily the case from (2.32). ∎

3. Second-order extension. Starting from a given first-order method, a common way to obtain a second-order extension is, as was already mentioned for the analogy with our hydrostatic reconstruction, to compute the fluxes from limited reconstructed values on both sides of each interface rather than cell-centered values; see [12], [23], or [30]. These new values are classically obtained with three ingredients: prediction of the gradients in each cell, linear extrapolation, and limitation procedure.

In the presence of a source and in the context of well-balanced schemes, this approach needs to be described in more detail. In particular, according to [20], [19], [7], since not only the reconstructed values $U_{i,r}$ at $i+1/2-$ and $U_{i+1,l}$ at $i+1/2+$ need to be defined but also $z_{i,r}$, $z_{i+1,l}$, a cell-centered source term S_{ci} must by added to preserve the consistency. We remark that even if z_i do not depend on time, the reconstructed values $z_{i,l}$, $z_{i,r}$ could depend on time via a coupling with U_i in the reconstruction step. Once these second-order reconstructed values are known, we apply the hydrostatic reconstruction scheme exposed in the previous section at each interface. This gives the second-order well-balanced scheme

$$\Delta x_i \frac{d}{dt} U_i(t) + F_{i+1/2} - F_{i-1/2} = S_i + S_{ci}, \tag{3.1}$$

where

$$F_{i+1/2} = \mathcal{F}(U_{i+1/2-}, U_{i+1/2+}), \tag{3.2}$$

$$U_{i+1/2-} = \begin{pmatrix} h_{i+1/2-} \\ h_{i+1/2-}\ u_{i,r} \end{pmatrix}, \qquad U_{i+1/2+} = \begin{pmatrix} h_{i+1/2+} \\ h_{i+1/2+}\ u_{i+1,l} \end{pmatrix}, \tag{3.3}$$

and the hydrostatic reconstruction is now

$$h_{i+1/2-} = \max(0, h_{i,r} + z_{i,r} - z_{i+1/2}), \qquad h_{i+1/2+} = \max(0, h_{i+1,l} + z_{i+1,l} - z_{i+1/2}), \tag{3.4}$$

with

$$z_{i+1/2} = \max(z_{i,r}, z_{i+1,l}). \tag{3.5}$$

The source term is distributed as before at the interfaces,

$$S_i = S_{i+1/2-} + S_{i-1/2+}, \tag{3.6}$$

$$S_{i+1/2-} = \begin{pmatrix} 0 \\ \frac{g}{2} h_{i+1/2-}^2 - \frac{g}{2} h_{i,r}^2 \end{pmatrix}, \quad S_{i-1/2+} = \begin{pmatrix} 0 \\ \frac{g}{2} h_{i,l}^2 - \frac{g}{2} h_{i-1/2+}^2 \end{pmatrix}. \tag{3.7}$$

A simple well-balanced choice for the centered source term S_{ci} is

$$S_{ci} = \begin{pmatrix} 0 \\ g \frac{h_{i,l}+h_{i,r}}{2} (z_{i,l} - z_{i,r}) \end{pmatrix}. \tag{3.8}$$

Using the definitions of the left and right numerical fluxes $\mathcal{F}_l$, $\mathcal{F}_r$ in (2.16), a compact formulation of the scheme is

$$\Delta x_i \frac{d}{dt} U_i(t) + \mathcal{F}_l(U_{i,r}, U_{i+1,l}, z_{i,r}, z_{i+1,l}) - \mathcal{F}_r(U_{i-1,r}, U_{i,l}, z_{i-1,r}, z_{i,l}) = S_{ci}. \tag{3.9}$$

This formulation ensures that the second-order scheme inherits the stability properties of the first-order one.

THEOREM 3.1. *Consider a consistent numerical flux $\mathcal{F}$ for the homogeneous problem that preserves nonnegativity of $h_i(t)$. Assume that the second-order reconstruction gives nonnegative values $h_{i,l}$, $h_{i,r}$, is well-balanced, and is second-order-centered in z, which means by definition that whenever the sequences (U_i) and (z_i) are the cell averages of smooth functions $U(x)$, $z(x)$, we have*

$$\begin{aligned} z_{i+1,l} - z_{i,r} &= O\left((\Delta x_i + \Delta x_{i+1})^3\right), \\ \frac{z_{i,r} - z_{i,l}}{\Delta x_i} &= z_x(x_i) + O\left((\Delta x_{i-1} + \Delta x_i + \Delta x_{i+1})^2\right). \end{aligned} \tag{3.10}$$

Then the finite volume scheme (3.1)–(3.8) *preserves the nonnegativity of $h_i(t)$, is well-balanced, i.e., preserves the steady states of a lake at rest* (2.3)*, and is second-order accurate.*

Proof. It is well known that the second-order reconstruction strategy preserves the nonnegativity of the water height (under a half CFL condition in the fully discrete case). Here only the centered source term S_{ci} in (3.9) could cause difficulties, but it does not since its first component vanishes.

The preservation of the lake-at-rest steady states can be checked easily from the property of the second-order reconstruction to be well-balanced, which means by definition that if $u_i = 0$ and $h_i + z_i = h_{i+1} + z_{i+1}$ for all i, then $u_{i,l} = u_{i,r} = 0$ and $h_{i,l} + z_{i,l} = h_{i,r} + z_{i,r} = h_i + z_i$ for all i. Indeed we just have to notice that for a steady state, $S_{ci} = (0, g(h_{i,r}^2 - h_{i,l}^2)/2)$.

In order to prove the second-order accuracy, let us assume that (U_i) and (z_i) are realized as the cell averages of smooth functions $U(x)$ and $z(x)$, and denote by $\hbar$ the mesh size. Then, since we assumed implicitly that the second-order reconstruction is second-order, we have that $U_{i,r} = U(x_{i+1/2}) + O(\hbar^2)$, $U_{i+1,l} = U(x_{i+1/2}) + O(\hbar^2)$, $z_{i,r} = z(x_{i+1/2}) + O(\hbar^2)$, $z_{i+1,l} = z(x_{i+1/2}) + O(\hbar^2)$. It follows from (3.3)–(3.5) that $U_{i+1/2\pm} = U(x_{i+1/2}) + O(\hbar^2)$, and thus by (3.2) $F_{i+1/2} = F(U(x_{i+1/2})) + O(\hbar^2)$. This proves the second-order accuracy in the weak sense of the flux difference in (3.1) since this part is in conservative form. For the right-hand side, there is no such cancellation, and thus we can only allow errors in $O(\Delta x_i \hbar^2)$ in (3.1). We have $(h_{i,l}+h_{i,r})/2 = h(x_i)+O(\hbar^2)$, and the second expansion in (3.10) yields with (3.8) that $S_{ci} = \big(0, -gh(x_i)z_x(x_i)\Delta x_i + O(\Delta x_i \hbar^2)\big) = \int_{x_{i-1/2}}^{x_{i+1/2}} (0, -gh(x)z_x(x))\,dx + O(\Delta x_i \hbar^2)$. Since $S_{i+1/2\pm} = O(z_{i+1,l} - z_{i,r}) = O(\hbar^3)$ by the first expansion in (3.10), this gives that $S_i = O(\hbar^3)$ and concludes the proof in the "regular" case when $\hbar = O(\Delta x_i)$ by just considering S_i as an error in (3.1). In the general case, we have to introduce a slightly different interpretation of the scheme via a weighted average flux

$$\widetilde{F}_{i+1/2} = \frac{\Delta x_{i+1}\mathcal{F}_l + \Delta x_i \mathcal{F}_r}{\Delta x_i + \Delta x_{i+1}} = F_{i+1/2} + \frac{\Delta x_i S_{i+1/2+} - \Delta x_{i+1} S_{i+1/2-}}{\Delta x_i + \Delta x_{i+1}}. \tag{3.11}$$

By the first line in (3.10), we have $\widetilde{F}_{i+1/2} = F_{i+1/2} - S_{i+1/2-} + O(\Delta x_i \hbar^2)$ and also $\widetilde{F}_{i+1/2} = F_{i+1/2} + S_{i+1/2+} + O(\Delta x_{i+1} \hbar^2)$. Therefore,

$$\begin{aligned} \widetilde{F}_{i+1/2} - \widetilde{F}_{i-1/2} &= F_{i+1/2} - F_{i-1/2} - S_{i+1/2-} - S_{i-1/2+} + O(\Delta x_i \hbar^2) \\ &= F_{i+1/2} - F_{i-1/2} - S_i + O(\Delta x_i \hbar^2), \end{aligned} \tag{3.12}$$

and (3.1) can be rewritten as

$$\Delta x_i \frac{d}{dt} U_i(t) + \widetilde{F}_{i+1/2} - \widetilde{F}_{i-1/2} = S_{ci} + O(\Delta x_i \hbar^2), \tag{3.13}$$

which proves the second-order accuracy. □

Some important features arising in the second-order reconstruction must now be specified. First, the cell-by-cell reconstruction preserves the mass conservation property of the finite volume method. Second, the limitation procedure ensures the nonnegativity of the second-order reconstructed water heights. The third important point is that the second-order reconstruction has to preserve the lake-at-rest steady state. To ensure this property we reconstruct also the bottom topography $z(x)$ although it is a data. The idea to do so is not so new (see [22], [11]), but here we give details on the more stable way to do it. Indeed only two of the three quantities $h, z, h+z$ need be explicitly reconstructed, the last being necessarily a combination of the other two. A critical test for making the right choice is given by considering a lake at rest with nonvertical shores, that is, considering only an interface between a wet cell and a dry cell in the case where the bottom of the dry cell is higher than the free surface in the wet cell and where the fluid is at rest in the wet cell. As it appears in Figure 1, for the minmod reconstruction, the only choice which preserves the steady state *and* the nonnegativity of the water height at a wet-dry interface is to work with the quantities h and $h + z$. Notice that it follows that in some respect the bottom topography changes at each timestep. This choice is consistent with the strategy for second-order extensions of a well-balanced Godunov-type scheme to multidimensional compressible flow under gravity in [5], [6] in that the *deviations from the nonconstant steady state* form the basis for reconstruction and slope limiting (even if this rule does not exclude the worst choice in the context of a wet-dry interface, namely, to reconstruct z and $h + z$). It is obvious then that the chosen second-order reconstruction preserves also the steady state in the classical case of wet-wet interfaces since we explicitly reconstruct the quantity $h+z$. The second-order-centered condition (3.10) can be realized, for example, with a second-order ENO reconstruction, but in practice we shall not do so because it becomes too complicate for two-dimensional unstructured meshes, even if it necessarily means a slight loss of accuracy. Second-order accuracy in time can be obtained as usual by a convex two-step integration of (3.9), and the CFL condition need not be modified.

4. Numerical results. All numerical tests are performed with a kinetic solver for the homogeneous problem. This solver is based on the kinetic theory developed in [27] and has the advantage of keeping the water height nonnegative, of verifying a discrete in-cell entropy inequality, and of being able to compute problems with shocks or vacuum. First- and second-order in space computations are proposed, but only first-order in time is used.

4.1. One-dimensional assessments. We first illustrate that the hydrostatic reconstruction does not affect the robustness of the homogeneous solver. We present a very classical numerical test of a constant discharge transcritical flow with shock over a bump; see [15] for a complete presentation. In Figures 2 and 3, where 101 points are used, we observe good first- and second-order results for this test, the stiffness of which is well known. As we are far from a hydrostatic steady state, the results of the well-balanced and standard schemes are quite similar. Notice, however, that the well-balanced version is less affected—regardless of the order of resolution—than the standard scheme where the derivative of the bottom topography presents strong variations.

To exhibit the improvement due to the hydrostatic reconstruction we present now a quasi-stationary case first proposed by LeVeque in [24] which consists in computing small perturbations of the steady state of a lake at rest with a varying bottom

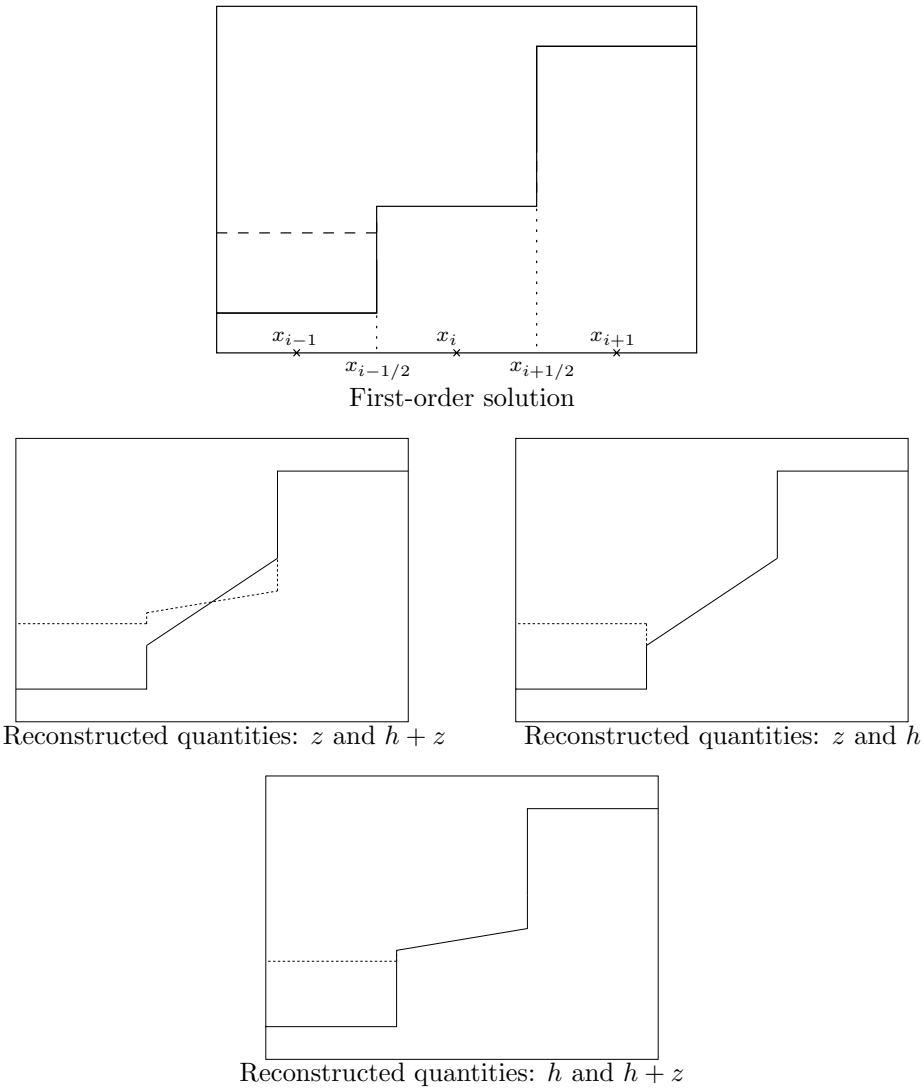

FIG. 1. *Second-order reconstruction strategy. Free surface (dotted line). Bottom topography (continuous line).*

topography:

$$z(x) = (0.25\,(\cos(\pi(x-1.5)/0.1)+1))_+\,,$$
$$h(0,x) = 1. + 0.001\mathbb{1}_{1.1\le x\le 1.2}.$$

As we can see by considering linearized equations, the small perturbation simply moves to the right with a speed equal to $\sqrt{h(t,x)}$, i.e., $\sqrt{1-z(x)}$ at first-order approximation (gravity is equal to 1). We present in Figure 4 the results obtained at $t = 0.7s$ and with 150 points, with the well-balanced scheme on the right, and with the standard one on the left. Notice that the scale is not the same on both graphs. It appears that even for the second-order computation the unphysical perturbations induced by the standard scheme are larger than the initial perturbation of the free

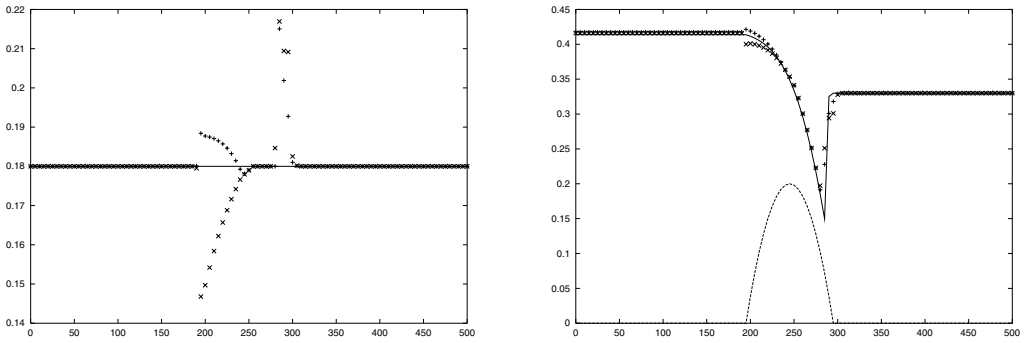

FIG. 2. *Constant discharge problem with shock: discharge and water height. First-order standard scheme (times crosses). First-order well-balanced scheme (plus crosses). Exact solution and bottom topography (solid and dotted lines).*

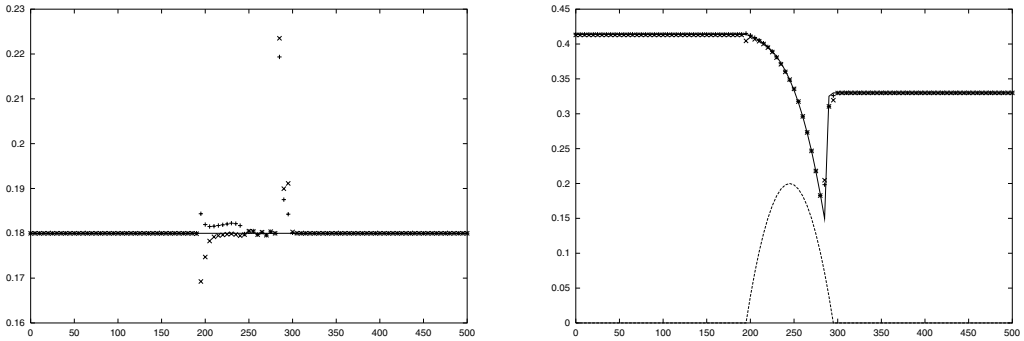

FIG. 3. *Constant discharge problem with shock: discharge and water height. Second-order standard scheme (times crosses). Second-order well-balanced scheme (plus crosses). Exact solution and bottom topography (solid and dotted lines).*

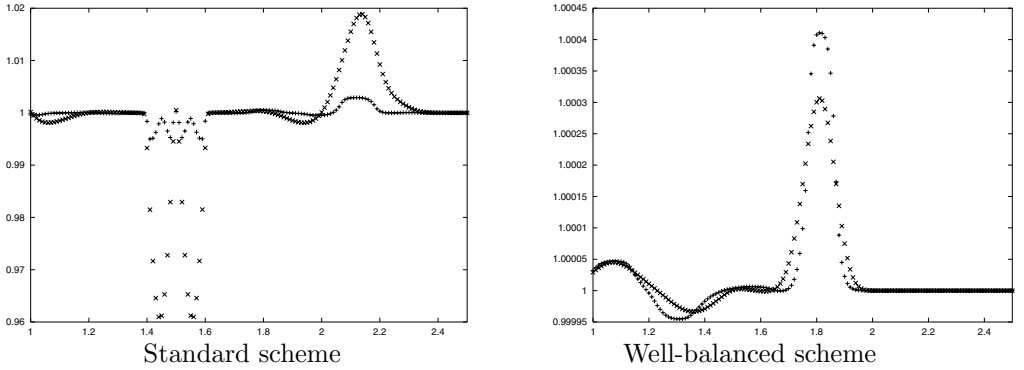

FIG. 4. *Quasi-stationary problem with small perturbation. First-order scheme (times crosses). Second-order scheme (plus crosses).*

surface. Moreover, the standard scheme induces not only a perturbation of the bump, but also a perturbation which moves to the right at the same speed as the initial perturbation, but which is more than one order of magnitude greater than the initial perturbation. On the contrary, the results obtained with the well-balanced scheme

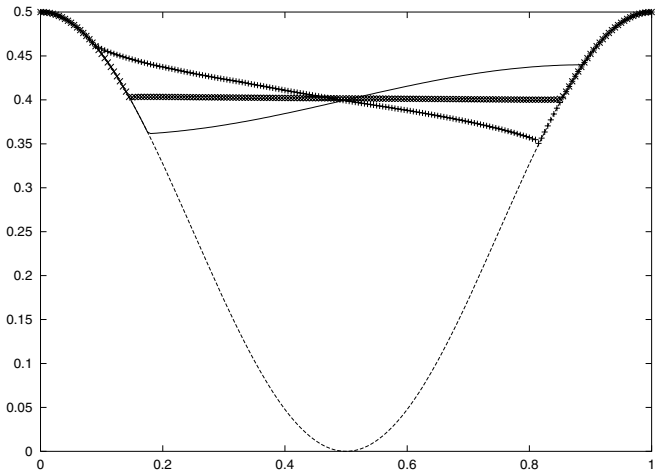

FIG. 5. *Oscillating lake: well-balanced scheme. First-order scheme (times crosses). Second-order scheme (plus crosses). Initial solution and bottom topography (solid and dotted lines).*

are good, even for the first-order solution.

To finish our assessment of scheme performance in one space dimension, we present a test case which is indicative of the robustness of a solver, as it involves vacuum conditions. It exhibits very clearly the improvement due to the second-order extension. We are interested in the case of an oscillating lake with a nonflat bottom and nonvertical shores. The lake is initially at rest, but a small sinusoidal perturbation affects the free surface:

$$z(x) = .5(1 - .5(\cos(\pi(x - .5)/.5) + 1)),$$
$$h(0, x) = \max(0, .4 - z(x) + .04\sin((x - .5)/.25) - \max(0, -.4 + z(x))).$$

Then the flow oscillates, and at each timestep we have to treat an interface between a wet cell and a dry cell on each shore of the lake. We present in Figure 5 the results obtained with the well-balanced scheme with 200 points at $t = 19.87s$, because it corresponds to a time where the flow reaches its higher level on the left shore. Both first- and second-order well-balanced schemes are robust, but the first-order scheme damps the oscillations much faster; fifty oscillations are enough to get back to rest. On the other hand the second-order well-balanced scheme keeps the periodic regime up to the machine accuracy.

4.2. Two-dimensional assessments. As the extension to second-order accuracy, the extension to the bidimensional case does not modify the idea of the method. The one-dimensional solver is used at each cell interface, and we have a numerical flux on each side of the interface, which are computed by $\mathcal{F}_l$ and $\mathcal{F}_r$ in (2.16) after an appropriate rotation. In this way, a piece of the source term is naturally discretized at the interface. The scheme is automatically well-balanced in the sense that lake-at-rest steady states $u = 0$, $h + z = cst$ are exactly preserved, and the water height remains nonnegative. However, some specific problems arise, especially in the construction of a two-dimensional well-balanced second-order scheme. We refer to [1], [2] for a detailed description, especially for the explanation of the two-dimensional hydrostatic second-order reconstruction.

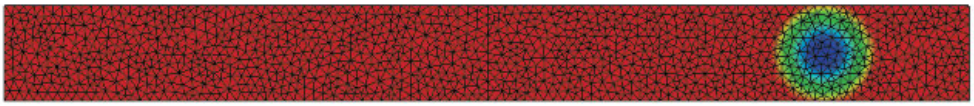

Mesh and bottom topography

Water height - Initial Solution

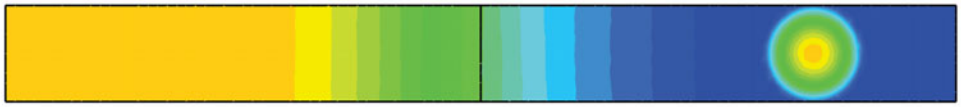

Water height - Solution at t=.08s

Water height - Solution at t=.16s

Scale for the water height

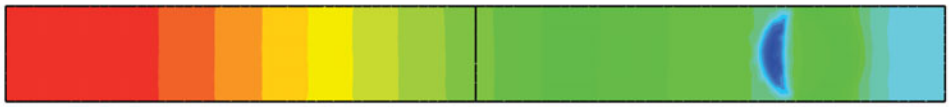

Free surface - Solution at t=.16s

Scale for the free surface level

FIG. 6. *Two-dimensional dam break on dry bed with a lake-at-rest area.*

We first present the academic case of a dam break on a dry bed but containing a wet zone which consists of a small lake at rest. This case involves the vacuum and allows us to exhibit the effect of the hydrostatic reconstruction to preserve the initially at rest area. The first subfigure in Figure 6 presents the mesh and the bottom topography. The bottom topography of the lake we can see on the right is hemispheric. On the second subfigure we can see the initial water height: we see the dam in the middle and the small lake at rest on the right. The free surface level in the lake coincides with the reference level of the bottom topography of the river, i.e., $(h + z)(0, x, y) = 0$ everywhere on the right of the dam. On the third subfigure we can see the rarefaction wave. Since it does not yet reach the lake, the steady state is

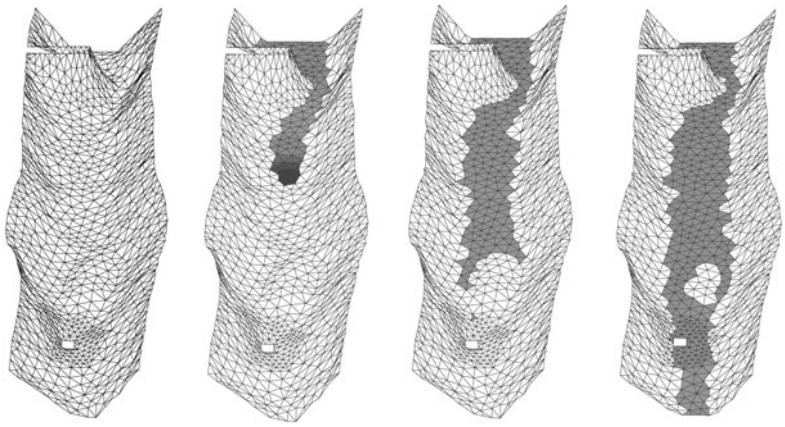

FIG. 7. *Filling up of a river. Bottom topography and free surface at different times.*

preserved. Then on the fourth subfigure the rarefaction wave reaches the lake and the water begins to move. On the last subfigure is presented the free surface level at this final time. We can notice strong variations on the lake area which lead to the formation of a hole in the left part of the lake (dark crescent), and a bump in the right part.

Then we present in Figure 7 another two-dimensional numerical test corresponding to the filling up of a river. This test still involves a vacuum but also deals with complex realistic geometry and bottom topography since it takes into account (i) a jetty in the transversal direction, in the upper part of the figures; (ii) a bridge pillar, the square on the lower part; and (iii) a small bump in the bottom topography. We start with an empty river and we prescribe a given water level as the inflow condition. On the first subfigure are presented the mesh and the associated bottom topography. Then we can notice that the strong variations in the bottom topography due to the jetty or the pillar bridge do not affect the robustness of the computation. On the third and fourth subfigures we can see the bump since the water skirts it.

More results can be found in [1], [10], [28], [26], and in [8] with the Coriolis force.

REFERENCES

[1] E. AUDUSSE, M.-O. BRISTEAU, AND B. PERTHAME, *Kinetic Schemes for Saint-Venant Equations with Source Terms on Unstructured Grids*, Report RR-3989, INRIA Rocquencourt, Le Chesnay, France, 2000; available online from http://www.inria.fr/rrrt/rr-3989.html.

[2] E. AUDUSSE, M.-O. BRISTEAU, AND B. PERTHAME, *Second Order Kinetic Scheme for Saint-Venant Equations with Source Terms on Unstructured Grids*, preprint.

[3] D. S. BALE, R. J. LEVEQUE, S. MITRAN, AND J. A. ROSSMANITH, *A wave propagation method for conservation laws and balance laws with spatially varying flux functions*, SIAM J. Sci. Comput., 24 (2002), pp. 955–978.

[4] R. BOTCHORISHVILI, B. PERTHAME, AND A. VASSEUR, *Equilibrium schemes for scalar conservation laws with stiff sources*, Math. Comp., 72 (2003), pp. 131–157.

[5] N. BOTTA, R. KLEIN, S. LANGENBERG, AND S. LÜTZENKIRCHEN, *Well-balanced finite volume methods for nearly hydrostatic flows*, J. Comput. Phys., submitted. (See also PIK-report 84, Potsdam Institute for Climate Impact Research, Potsdam, Germany, available online from http://www.pik-potsdam.de/reports.)

[6] N. BOTTA, R. KLEIN, AND A. OWINOH, *Distinguished limits, multiple scales asymptotics, and numerics for atmospheric flows*, in Proceedings of the 13th International Conference on Atmosphere-Ocean Fluid Dynamics, Breckenridge, CO, American Meteorological Society, Boston, MA, 2001.

[7] F. Bouchut, *Nonlinear Stability of Finite Volume Methods for Hyperbolic Conservation Laws, and Well-Balanced Schemes for Sources*, Frontiers in Math., Birkhäuser, 2004.
[8] F. Bouchut, J. LeSommer, and V. Zeitlin, *Frontal geostrophic adjustment and nonlinear-wave phenomena in one dimensional rotating shallow water. Part* 2: *High resolution numerical investigation*, J. Fluid Mech., to appear.
[9] F. Bouchut, A. Mangeney-Castelnau, B. Perthame, and J.-P. Vilotte, *A new model of Saint-Venant and Savage-Hutter type for gravity driven shallow water flows*, C. R. Acad. Sci. Paris Sér. I Math., 336 (2003), pp. 531–536.
[10] M.-O. Bristeau and B. Coussin, *Boundary conditions for the shallow water equations solved by kinetic schemes*, Report RR-4282, INRIA Rocquencourt, Le Chesnay, France, 2001; available online from http://www.inria.fr/rrrt/rr-4282.html.
[11] T. Gallouët, J.-M. Hérard, and N. Seguin, *Some approximate Godunov schemes to compute shallow-water equations with topography*, Computers and Fluids, 32 (2003), pp. 479–513.
[12] E. Godlewski and P.-A. Raviart, *Numerical Approximation of Hyperbolic Systems of Conservation Laws*, Appl. Math. Sci. 118, Springer-Verlag, New York, 1996.
[13] L. Gosse, *A well-balanced flux-vector splitting scheme designed for hyperbolic systems of conservation laws with source terms*, Comput. Math. Appl., 39 (2000), pp. 135–159.
[14] L. Gosse and A.-Y. LeRoux, *A well-balanced scheme designed for inhomogeneous scalar conservation laws*, C. R. Acad. Sci. Paris Sér. I Math., 323 (1996), pp. 543–546.
[15] N. Goutal and F. Maurel, *Proceedings of the Second Workshop on Dam-Break Wave Simulation*, Technical report EDF/DER HE-43/97/016/B, Châtou, France, 1997.
[16] J. M. Greenberg and A.-Y. LeRoux, *A well-balanced scheme for the numerical processing of source terms in hyperbolic equations*, SIAM J. Numer. Anal., 33 (1996), pp. 1–16.
[17] E. Isaacson and B. Temple, *Convergence of the* 2×2 *Godunov method for a general resonant nonlinear balance law*, SIAM J. Appl. Math., 55 (1995), pp. 625–640.
[18] S. Jin, *A steady-state capturing method for hyperbolic systems with geometrical source terms*, Math. Model. Numer. Anal., 35 (2001), pp. 631–645.
[19] T. Katsaounis, B. Perthame, and C. Simeoni, *Upwinding Sources at Interfaces in conservation laws*, Appl. Math. Lett., to appear.
[20] T. Katsaounis and C. Simeoni, *First and Second Order Error Estimates for the Upwind Interface Source Method*, preprint.
[21] A.-Y. LeRoux, *Riemann solvers for some hyperbolic problems with a source term*, in Actes du 30ème Congrès d'Analyse Numérique: CANum '98 (Arles, 1998), ESAIM Proc. 6, Soc. Math. Appl. Indust., Paris, 1999, pp. 75–90.
[22] A.-Y. LeRoux, *Discrétisation des termes sources raides dans les problèmes hyperboliques*, in Systèmes hyperboliques: Nouveaux schémas et nouvelles applications. Ecoles CEA-EDF-INRIA "problèmes non linéaires appliqués," INRIA Rocquencourt, Le Chesnay, France, 1998; available online from http://www-gm3.univ-mrs.fr/~leroux/publications/ay.le_roux.html.
[23] R. J. LeVeque, *Finite Volume Methods for Hyperbolic Problems*, Cambridge University Press, Cambridge, UK, 2002.
[24] R. J. LeVeque, *Balancing source terms and flux gradients in high-resolution Godunov methods: The quasi-steady wave-propagation algorithm*, J. Comput. Phys., 146 (1998), pp. 346–365.
[25] T.-P. Liu, *Nonlinear resonance for quasilinear hyperbolic equation*, J. Math. Phys., 28 (1987), pp. 2593–2602.
[26] A. Mangeney, J.-P. Vilotte, and M.-O. Bristeau, B. Perthame, C. Simeoni, and S. Yernini, *Numerical Modeling of Avalanches Based on Saint-Venant Equations Using a Kinetic Scheme*, preprint.
[27] B. Perthame, *Kinetic Formulations of Conservation Laws*, Oxford University Press, London, 2002.
[28] B. Perthame and C. Simeoni, *A kinetic scheme for the Saint-Venant system with a source term*, Calcolo, 38 (2001), pp. 201–231.
[29] B. Perthame and C. Simeoni, *Convergence of the upwind Interface source method for hyperbolic conservation laws*, in Proceedings of Hyp2002, T. Hou and E. Tadmor, eds., Springer-Verlag, Berlin, 2003.
[30] E. F. Toro, *Riemann Solvers and Numerical Methods for Fluid Dynamics. A Practical Introduction*, 2nd ed., Springer-Verlag, Berlin, 1999.
[31] M. E. Vazquez-Cendon, *Improved treatment of source terms in upwind schemes for the shallow water equations in channels with irregular geometry*, J. Comput. Phys., 148 (1999), pp. 497–526.
[32] K. Xu, *A well-balanced gas-kinetic scheme for the shallow water equations with source terms*, J. Comput. Phys., 178 (2002), pp. 533–562.